Journal of Atmospheric and Solar–Terrestrial Physics 149 (2016) 46–51

Contents lists available at ScienceDirect

Journal of Atmospheric and Solar–Terrestrial Physics

journal homepage: www.elsevier.com/locate/jastp

Phase synchronization between tropospheric radio refractivity and rainfall amount in a tropical region

Ibiyinka A. Fuwape, Samuel T. Ogunjo*, Joseph B. Dada, Gabriel A. Ashidi, Israel Emmanuel

Department of Physics, Federal University of Technology, Akure, Nigeria

ARTICLE INFO

Keywords:
Phase synchronization
Radio refractivity
Precipitation
Recurrence plot
RQA
Climate

ABSTRACT

This study investigated linear and nonlinear relationship between the amount of rainfall and radio refractivity in a tropical country, Nigeria using forty seven locations scattered across the country. Correlation and Phase synchronization measures were used for the linear and nonlinear relationship respectively. Weak correlation and phase synchronization was observed between seasonal mean rainfall amount and radio refractivity while strong phase synchronization was found for the detrended data suggesting similar underlying dynamics between rainfall amount and radio refractivity. Causation between rainfall and radio refractivity in a tropical location was studied using Granger causality test. In most of the Southern locations, rainfall was found to Granger cause radio refractivity. Furthermore, it was observed that there is strong correlation between mean rainfall amount and the phase synchronization index over Nigeria. Coupling between rainfall and radio refractivity has been found to be due to water vapour in the atmosphere. Frequency planning and budgeting for microwave propagation during periods of high rainfall should take into consideration this nonlinear relationship.

1. Introduction

Exponential growth in radio communication needs has necessitated the demand for more bandwidths for communication (Adedayo et al., 2013). Possibilities of high and low frequencies are being investigated to meet the growing demands. Satellite communications systems are designed with several factors such as fading, noise, cross polarization etc. in mind. Several factors such as soil parameters (Adedayo et al., 2013), cloud, and rainfall affect signal propagation in communication systems. Liquid Water Content (LWC) of clouds has been reported to contribute about 0.8% to the total refractivity in the troposphere (Yang and Zou, 2012). The contributions of hydrometeors, water vapour, dry air and other particulate to propagation have been reported by Solheim et al. (1999). The path delay (ZD) can be computed using the expression $ZD\,(mm) = \int_0^\infty N dz$, where N is the refractivity and z is the vertical signal path in kilometers (Solheim et al., 1999; Hogg et al., 1981). To account for the effect of rainrate (R) on attenuation (A) of radio signals in the troposphere, Olsen et al. (1978) proposed a relationship of the form $A = aR^b$ where a and b are functions of transmitting frequency and rain temperature. However, propagation of electromagnetic waves in the troposphere (about 10 km) altitude above the earth surface is affected by two key factors: precipitation and variations in refractivity.

Rainfall is very important to the existence of man. It plays important role in determining the economy of a location. Excessive rainfall causes ecological disasters while insufficient rainfall makes a location unsuitable for existence. Rainfall has been described as one of the most complex and difficult components of the hydrological cycle to model (Maity, 2012). Rainfall interferes or attenuates communication signals, making it an important factor to be considered in frequency planning. The attenuation of signals due to rain becomes very significant at frequencies above 10 GHz, especially in the tropics (Das and Maitra, 2012). Rain rate, freezing height, rainfall type and drop size are properties of rainfall that has effect on communication and communication systems (Kof et al., 2014; Ojo et al., 2010).

Refraction is the bending of waves as it passes through different media. Refractivity is defined as the refractive index of air (Adeyemi and Emmanuel, 2011). Refractivity N has two components (1); hydrostatic or dry component N_{dry} and the non-hydrostatic or wet component N_{wet} (Raju et al., 2007). Consequences of radio refractivity include multipath fading, interference, attenuation due to difraction on the terrain obstacles, radio hole, e.t.c. Tropospheric refractivity has been reported to experience diurnal and seasonal variations with strong dependence on temperature inversion and humidity (Adediji et al., 2015). Vertical gradient of radio refractivity helps in quantifying anomalous propagation phenomena such as super refraction, sub

* Corresponding author.
E-mail addresses: iafuwape@futa.edu.ng (I.A. Fuwape), stogunjo@futa.edu.ng (S.T. Ogunjo), jbinaction2003@yahoo.com (J.B. Dada), agashidi@futa.edu.ng (G.A. Ashidi), iemmanuel@futa.edu.ng (I. Emmanuel).

http://dx.doi.org/10.1016/j.jastp.2016.09.009
Received 7 April 2016; Received in revised form 26 August 2016; Accepted 21 September 2016
Available online 28 September 2016
1364-6826/

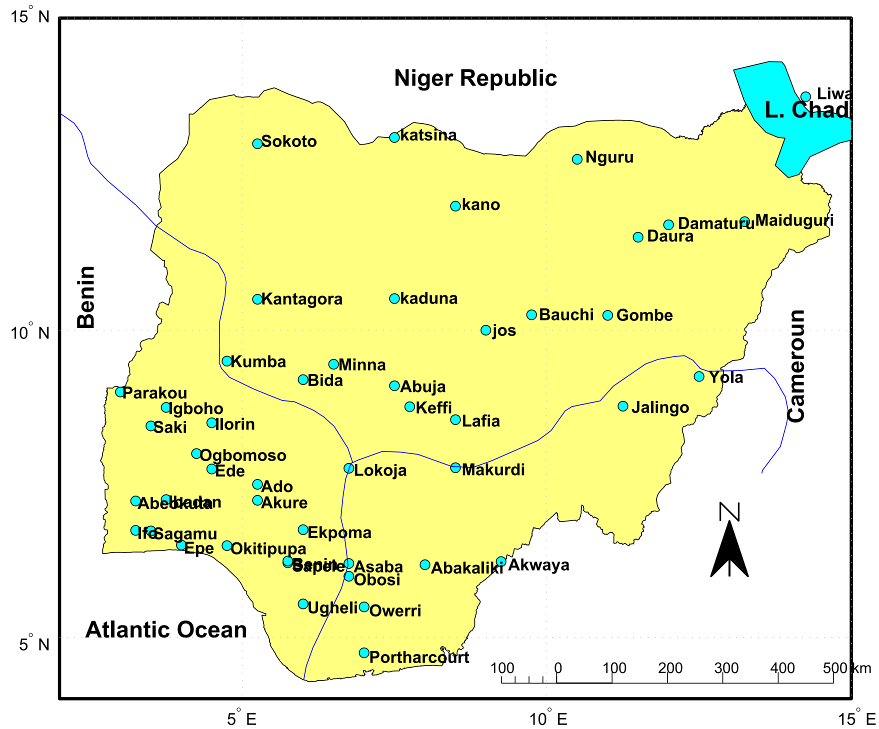

Fig. 1. Map of Nigeria showing the study locations.

refraction and ducting which have significant effects on the propagating signals Under ducting, signals become trapped or guided between layers of the atmosphere and the signal is obtained at a very long range (far beyond the receiver).

$$N_{dry} = 77.6\frac{P}{T} \tag{1}$$

$$N_{wet} = 6.48\frac{e}{T} + 3.75 \times 10^5\frac{e}{T^2} \tag{2}$$

where P, T and e are the pressure (hPa), temperature (K) and water vapour (hPa) (Midya et al., 2013; Bevis et al., 1994). The largest contribution to the atmospheric delay is the hydrostatic constituents (L_D) followed by water vapour induced delay (L_V).

Rainfall (Ogunjo et al., 2015) and refractivity (Adeyemi and Emmanuel, 2011) shows strong seasonal variations in the tropics. The months of March - September marks the wet season in the tropics. In Nigeria, three (3) wind currents, viz. the tropical maritime air mass, the tropical continental air mass and the equatorial easterlies, controls the climate. The tropical maritime, which originates from the Namibian coast is responsible for the wet season in the country. During this period, rainfall amount and intensity are high and values of refractivity are high. From October to February, low values of rainfall amount and refractivity are recorded. Due to the effect of Intertropical Discontinuity, the month of August has low frequency of rainfall and consequently results in low refractivity values. High values of refractivity during the rainy season has been attributed to the high air humidity commonly observed in the tropics during the wet season (Adediji and Ajewole, 2008). Also, nonlinearity has been reported in the underlying dynamics of both rainfall (Sharifi et al., 1990; Shirer et al., 1997) and refractivity time series (Adediji and Ogunjo, 2014; Ogunjo et al., 2014). Similarities between the distribution pattern of these rainfall amount and radio refractivity suggest the need to investigate the statistical significance of the relationship between them.

Depending on the complexities between two time series (rainfall amount and radio refractivity), the relationship between them can be linear or nonlinear. Linear relationship can be investigated using correlation or regression analysis. Correlation quantifies the strength of a linear relationship between two variables. Pearson and Spearman correlation are the two most commonly used correlation estimates, $r(-1 \le r \le +1)$. Closeness to +1 and −1 represent positive and negative relationship respectively. According to Legates and McCabe (1999), the use of correlation and correlation based measures in hydrological and hydroclimatic models is influenced by extreme values (outliers). However, correlation between two variables does not indicate causation of one by the other. The fact that X_t correlates well with Y_t does not imply that changes in X_t can be used to predict a change in Y_t. The Granger causality test can be used to investigate, if there exist, a dynamic relationship between two variables. If some other series Y_t, contains information in past terms that helps in the prediction of X_t, and if this information is contained in no other series used in the predictor, then Y_t is said to cause X_t (Granger, 1969). Two commonly used methods for the computation of Granger causality are "Granger Direct Method" and Haugh-Pierce approach (Freeman, 1983). The Granger Direct Method is based on regression while the Haugh-Pierce approach uses an ARIMA model for each series. This approach is very sensitive to choice of lag length and cannot tell the direction of causality.

Pikovsky et al. (2003) defines synchronization as the adjustment of rhythms of oscillating objects due to their interaction. According to Boccaletti et al. (2002), synchronization of chaotic systems can be defined as a process where two (or many) chaotic systems (either equivalent or nonequivalent) adjust a given property of their motion to a common behavior, due to coupling or forcing. This ranges from complete agreement of trajectories to locking of phases. Synchronization was first observed in coupled pendulum by Huygens. Quantitative investigation of synchronization of nonlinear system was pioneered by Pecora and Carroll (1990) for two systems described by a set of differential equations. Due to its relevance to several fields of studies, the field has grown to include different types of synchronization (Ojo and Ogunjo, 2012; , 2014b). However, there exist several natural occurring time series that exhibit a form of synchronization. Some examples of such systems as described by Boccaletti et al. (2002) include: the human cardiorespiratory system, an extended ecological system, the magnetoencephalographic activity of Parkinsonian pa-

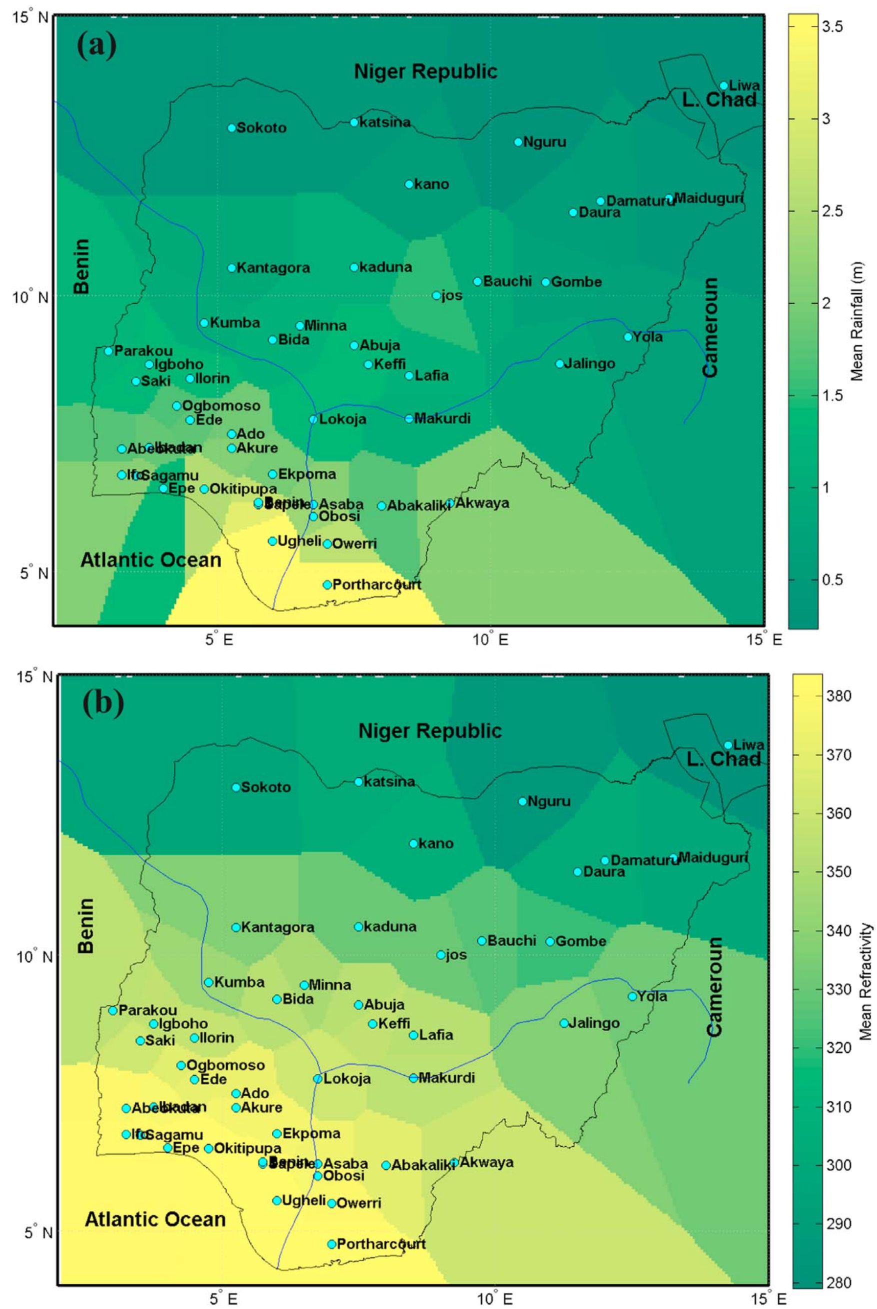

Fig. 2. Mean rainfall amount and refractivity values across the country during the period 1979–2014.

tients, the electrosensitive cells of the paddlefish, the sunspot cycle and a fast component of the solar inertial motion and synchronization phenomena in nephron - nephron interaction in rat kidneys.

The different types of synchronization developed over the years include: lag synchronization, phase synchronization, complete synchronization, projective synchronization and anticipated synchronization (Ojo et al., 2014c; Ogunjo, 2013). When two time series or trajectories change their course in same way, even at different time, they may be thought as phase synchronous. More generally, if they do not change in the same way, but maintain a constant ratio in course of their alteration, they can still be thought as phase synchronized or phase locked or phase coupled (Majumdar, 2006). An approach to investigate phase synchronization using recurrence plots was proposed by Marwan et al. (2007). A recurrence matrix is defined as:

$$R_{i,j} = \Theta(\varepsilon - \| x_i - x_j \|), \quad i, j = 1\ldots,N \tag{3}$$

where x_i stands for the point in phase space at which the system is situated at a time i, and ε is a predefined threshold, $\Theta(x)$ is the Heaviside function. For systems that are phase synchronized, the probability of recurrence will be maximal at the same time and phase synchronization index (CPR) will tend towards 1 (Marwan et al., 2007).

Rain and refractivity play an important role in communication systems. However, no investigation has been made into nonlinear relationship between the two parameters in a tropical station. This study aims to investigate linear and nonlinear relationship between rain and refractivity. The results would be useful in developing nonlinear models for the prediction of refractivity values that will help in radio frequency and communication budget planning in tropical

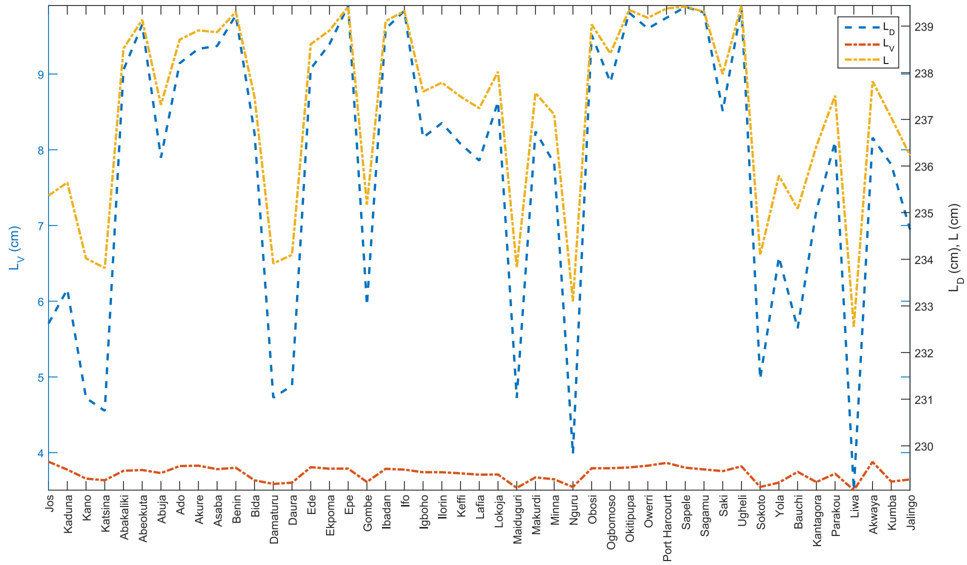

Fig. 3. Total phase delay, phase delay due to hydrostatic constituents and water vapour for each of the locations under consideration.

regions.

2. Methodology

2.1. Study area

The study area is Nigeria. Nigeria lies between 4–14°N and 3–15°E. Forty-seven (47) locations were chosen across the country for investigation. The positions of the locations are shown in Fig. 1..

2.2. Data analysis

Daily re-analysis data covering the period 1979–2014 was obtained from the European Centre for Medium-Range Weather Forecasts (ECMWF) Re-Analysis (ERA-Interim) project http://apps.ecmwf.int/datasets/data/interim-full-daily. Precipitation, 2 m dew point, 2 m temperature and pressure were extracted for the locations under consideration (Dee et al., 2011). Time series of rainfall amount and computed refractivity is shown in Fig. 2..

Relative humidity (RH) data was obtained from 2 m dew point temperature using the expression (Tetens, 1930)

$$RH = 100 - 5(t - t_d) \tag{4}$$

where t and t_d are the 2 m temperature and dew point respectively. Saturated water vapour pressure was computed from the expression (CCIR, 1986)

$$e_s = \left[\frac{5854}{T^5}\right]\left[10^{20-\frac{2950}{T}}\right] \tag{5}$$

where T is the absolute temperature in Kelvin. Using Eqs. (4) and (5), water vapour pressure e is obtained as (ITU-R, 1997)

$$e = \left(\frac{RH}{100} \times e_s\right) \tag{6}$$

Wet component of surface refractivity is then computed from the expression

$$N_w = 64.8\frac{e}{T} + 3.37 \times 10^5\frac{e}{T^2} \tag{7}$$

where P, T and e are the pressure (hPa), temperature (K) and water vapour (hPa) (Midya et al., 2013).

The individual contributions of L_V and L_D are computed using Hogg et al. (1981) expression

$$L_D = 0.2272P_{OD} \tag{8}$$

$$L_V = 6.50V \tag{9}$$

where V and P_{OD} are the precipitable water vapour and surface pressure in millibar respectively. The precipitable water vapour was computed using the expression by Reitan (1963)

$$\ln V = 0.1102 + 0.06138t_d \tag{10}$$

where t_d is the dew point temperature in °C. Results obtained for V is in very good agreement with those obtained for the same region by Adeyemi (2009).

2.3. Mathematical analysis

In this paper, the linear correlation between rainfall amount and refractivity values for all locations were computed using the Pearson correlation coefficient at 95% confidence interval, using the expression

$$r = \frac{\sum_{i=1}^{N}(x_i - \bar{x})(y_i - \bar{y})}{\sqrt{\sum_{i=1}^{N}(x_i - \bar{x})^2}\sqrt{\sum_{i=1}^{N}(y_i - \bar{y})^2}} \tag{11}$$

where $\bar{x}$, $\bar{y}$ are the sample mean and N is the sample size (Arora et al., 2012). Since $0's$ affect the correlation results, all non raining days (rainfall amount <0.001 mm) and corresponding wet refractivity values for those days were removed. Also, the data were differenced to remove trend and achieve stationarity (Ogunjo, 2015).

The Granger Direct method was employed in this work. Each of the variables rain (X_t) and radio refractivity (Y_t) were made stationary by differencing. A suitable lag (m) was obtained using the Bayesian Information Criterion (BIC). Using the value of m obtained, a model of the form (Granger, 1969)

$$Y_t = \alpha_0 + \sum_{j=1}^{m} a_j Y_{t-j} + \sum_{k=1}^{m} b_k X_{t-k} + \varepsilon_t X_t = \beta_0 + \sum_{j=1}^{m} c_j X_{t-j} + \sum_{k=1}^{m} d_k Y_{t-k} + \eta_t$$

where ε_t and η_t are two uncorrelated white noise time series. Y_t is causing X_t if some b_j is not zero. Similarly, X_t is causing Y_t if some c_j is not zero. Causation between the two time series in both direction indicates that a feedback mechanism exist between them (Granger, 1969). Test statistics such as F-test can be used to test the null hypothesis H_0 that Y Granger cause X. If The value of the F-statistics is greater than the critical value from the F-distribution, we reject the null hypothesis that Y does not Granger Cause X.

The phase synchronization index (CPR) were computed using the vertical distances which separate diagonal lines in an RP, and the time scales which characterize the dynamical system, as described by Marwan et al. (2007). The recurrence plots of the two time series are computed using Eq. (3). An indication of phase synchronization is the matching of the distances between the vertical diagonal lines of the recurrence plots. CPR is defined by Marwan et al. (2007) as the correlation between $p_{\tau}^{\bar{x}}$ and $p_{\tau}^{\bar{y}}$, i.e.

$$CPR = \langle \overline{p}^{\bar{x}}(\tau)\overline{p}^{\bar{y}}(\tau)\rangle \tag{12}$$

where $\overline{p}^{\bar{x}}(\tau)$ and $\overline{p}^{\bar{y}}(\tau)$ are the probabilities normalized to zero mean and standard deviation of one. A value close to one indicates phase synchronization. Phase synchronization index (ant its standard deviation) between rainfall amount and refractivity was computed yearly for each location under consideration. The results are shown in Table 1. Computation of phase synchronization index was done using the toolbox (http://www.agnld.uni-potsdam.de/marwan/toolbox) by Marwan et al. (2007).

3. Results and discussion

Rainfall and radio refractivity values for locations in the Northern part of the country are seen to have a lower mean rainfall amount when compared to locations in the Southern part of the country. This is largely due to the presence of the Atlantic Ocean that borders the Southern part of the country (Fig. 2). The Pearson correlation coefficient was used to investigate linear relationship between the rainfall amount and refractivity. The results obtained are shown in Table 1. All values are significant with $p \leq 0.05$. The correlation values are found to be in the range from 0.07 to 0.54 and 0.21-0.51 for the seasonal and detrended series, signifying positive but weak linear relationship between rainfall amount and radio refractivity. A linear regression analysis of rainfall amount and refractivity (not shown) reveals that a very weak linear relationship exist between the two parameters. From the Granger causality test, the null hypothesis is accepted for most of the stations in the Southern part of the country except for locations such as Ibadan, Ifo, Okitipupa, Port Harcourt and Sagamu. The rejection of the null hypothesis in these region can be attributed to local effects such as anthropogenic causes, land topography and high variability of rainfall in those places. The rejection of the null hypothesis in many of the northern locations is due to the extended dry season and very short rainfall period experienced in the region. The phase delay due to hydrostatic constituents, water vapour and total phase delay are shown for each location in Fig. 3. Higher phase delay were observed in the southern locations while lower values were obtained for the northern regions. This further supports the hypothesis that rain has a direct influence on radio refractivity. The hydrostatic component was found to account for about 95–98% of the total phase delay..

On the other hand, phase synchronization index (CPR) between rainfall amount and refractivity shows high values ranges 0.00–0.29 and 0.43–0.94 for the original and detrended data respectively, indicating stronger coupling in the detrended series than seasonal series. The stronger coupling in the detrended series indicates that both rainfall amount and wet component of refractivity have the same underlying dynamics or driving mechanism. It is observed using both seasonal and detrended data, that the value of phase synchronization is lower for northern regions compare to locations in the south of the country. Using Pearson correlation coefficient, there exist a positive correlation at 95% confidence interval $(0.60,\ \mathrm{p-value} < 0.05)$ between the mean rainfall amount in a location and the CPR index at that location. This implies that locations with higher mean rainfall amount synchronizes in phase with refractivity better than locations with lower mean rainfall amount. The level of synchronization between the two variables can be attributed to their coupling through atmospheric water vapour. Water vapour density is higher during the wet season than

Table 1
Pearson Correlation (r), Granger Casuality test and phase synchronization (CPR) between rainfall and wet component of radio refractivity over the study area.

Location	mean rainfall (m)	r	r[a]	H_0[a]	CPR	CPR[b]	CPR[a]	CPR[a,b]
Jos	0.0015	0.29	0.41	1	0.18	0.16	0.92	0.03
Kaduna	0.0011	0.35	0.41	1	0.17	0.15	0.89	0.05
Kano	0.0006	0.48	0.43	1	0.15	0.15	0.94	0.02
Katsina	0.0005	0.42	0.36	1	0.16	0.14	0.92	0.03
Abakaliki	0.0017	0.22	0.28	1	0.07	0.11	0.76	0.11
Abeokuta	0.0017	0.30	0.40	1	0.02	0.10	0.76	0.11
Abuja	0.0014	0.28	0.33	1	0.07	0.12	0.84	0.08
Ado	0.0020	0.24	0.33	1	0.00	0.11	0.85	0.06
Akure	0.0021	0.18	0.31	1	0.01	0.12	0.83	0.06
Asaba	0.0021	0.21	0.35	1	0.03	0.09	0.72	0.14
Benin	0.0021	0.17	0.32	1	0.01	0.12	0.69	0.16
Bida	0.0028	0.27	0.25	1	0.15	0.13	0.84	0.06
Damaturu	0.0012	0.43	0.36	0	0.26	0.16	0.94	0.02
Daura	0.0006	0.42	0.37	1	0.20	0.16	0.93	0.03
Ede	0.0006	0.26	0.34	1	0.03	0.11	0.84	0.07
Ekpoma	0.0018	0.21	0.36	1	0.01	0.11	0.77	0.11
Epe	0.0020	0.21	0.26	1	0.03	0.09	0.58	0.20
Gombe	0.0014	0.39	0.40	1	0.22	0.18	0.91	0.05
Ibadan	0.0007	0.29	0.38	0	0.02	0.08	0.78	0.09
Ifo	0.0007	0.39	0.49	0	0.04	0.12	0.66	0.16
Igboho	0.0018	0.28	0.31	1	0.24	0.17	0.87	0.07
Ilorin	0.0021	0.27	0.32	1	0.18	0.14	0.86	0.08
Keffi	0.0014	0.24	0.34	0	0.08	0.14	0.80	0.11
Lafia	0.0014	0.26	0.37	1	0.10	0.12	0.81	0.12
Lokoja	0.0007	0.35	0.40	0	0.08	0.10	0.75	0.12
Maiduguri	0.0014	0.43	0.32	1	0.22	0.15	0.93	0.03
Makurdi	0.0012	0.29	0.36	1	0.10	0.12	0.77	0.12
Minna	0.0013	0.24	0.28	0	0.06	0.12	0.83	0.08
Nguru	0.0005	0.54	0.46	1	0.17	0.14	0.91	0.03
Obosi	0.0011	0.12	0.28	1	0.00	0.13	0.71	0.14
Ogbomoso	0.0012	0.29	0.36	1	0.09	0.10	0.83	0.06
Okitipupa	0.0003	0.23	0.34	0	0.02	0.10	0.72	0.15
Owerri	0.0023	0.07	0.24	1	0.02	0.11	0.68	0.17
Port Harcourt	0.0017	0.09	0.24	0	0.01	0.08	0.43	0.21
Sapele	0.0026	0.13	0.29	1	0.03	0.12	0.64	0.19
Sagamu	0.0035	0.42	0.51	0	0.03	0.08	0.64	0.16
Saki	0.0021	0.26	0.32	1	0.18	0.15	0.85	0.07
Ugheli	0.0027	0.13	0.25	1	0.00	0.10	0.60	0.18
Sokoto	0.0035	0.47	0.43	0	0.14	0.16	0.92	0.03
Yola	0.0031	0.22	0.22	1	0.08	0.13	0.85	0.07
Bauchi	0.0021	0.33	0.35	0	0.21	0.15	0.91	0.06
Kantagora	0.0014	0.32	0.35	0	0.23	0.13	0.88	0.05
Parakou	0.0036	0.28	0.29	1	0.29	0.14	0.87	0.05
Liwa	0.0004	0.41	0.24	0	0.24	0.21	0.88	0.07
Akwaya	0.0007	0.24	0.26	1	0.08	0.11	0.87	0.06
Kumba	0.0020	0.20	0.21	0	0.20	0.14	0.88	0.05
Jalingo	0.0010	0.26	0.32	1	0.15	0.13	0.83	0.09

Note: r is the Pearson correlation coefficient, $H_0 = 1$ implies that Y Granger cause X while $H_0 = 0$ indicates that Y does not Granger cause X. Granger causality test was performed using a lag of 1.

[a] Represents result for differenced data.

[b] Indicates standard deviation of the parameter.

during the dry season for tropical locations (Adediji et al., 2015; Emmanuel et al., 2015; Ayoade, 1983). According to Adediji et al. (2015), water vapour pressure has the most significant influence on radio refractivity with both showing similar seasonal and peak/off-peak trends throughout the years and levels above the ground. Similarly, Emmanuel et al. (2015) reports that water vapour and rainfall follow the same seasonal trends. Furthermore, spatial trends in both refractivity and rainfall across the country can be explained in terms of water vapour. According to Ayoade (1983), provided water is available for evaporation and the air is warm the water vapour content of the atmosphere will be high. The Atlantic ocean presents a large body of water such that water vapour is high in the coastal region and reduces in value in the inland. This explains high rainfall amount and refractivity in the Southern part of the country.

4. Conclusion

This study has investigated the linear and nonlinear relationship between rainfall amount and radio refractivity across forty-seven (47) stations in a tropical country, Nigeria. Results indicate that linear relationship, using Pearson correlation coefficient, cannot fully capture the association between the two parameters investigated. Causation of radio refractivity by rainfall is confirmed in several locations within the country, especially in the southern part of the country. A nonlinear relationship, using phase synchronization index, is used to investigate a nonlinear relationship between the two parameters. They are found to have high CPR values. High variability was observed in the phase synchronization index when the seasonal trends in the data is removed. Coupling between the two parameters is attributed to water vapour pressure values. This relationship is seen to be enhanced in the southern part of the country which experiences more rainfall than the northern part of the country. Frequency planning and budgeting for microwave propagation during periods of high rainfall should take into consideration this nonlinear relationship. With increasing prediction accuracy for rainfall occurrences and amount, better prediction of radio refractivity can easily be made based on this nonlinear relationship.

References

Adedayo, K.D., Ajewole, M.O., Ogunjo, S.T., Agboola, O., 2013. Measurement of soil electrical parameters for planning AM and FM radio broadcast stations in Southwestern Nigeria. J. Niger. Assoc. Math. Phys. 23, 503–510.

Adediji, A.T., Ajewole, M.O., 2008. Vertical profile of radio refractivity gradient in akure south-west nigeria. Prog. Electromagn. Res. C 4, 157–168.

Adediji, A.T., Ajewole, M.O., Ojo, J.S., Ashidi, A.G., Ismail, M., Mandeep, J.S., 2015. Influence of some meteorological factors on tropospheric radio refractivity over a tropical location in nigeria. MAUSAM 66 (January (1)), 123–128.

Adediji, A.T., Ogunjo, S.T., 2014. Variations in non-linearity in vertical distribution of microwave radio refractivity. Prog. Electromagn. Res. M 36, 177–183, ⟨http://www.jpier.org/PIERM/pier.php?paper=14041606⟩.

Adeyemi, B., 2009. Empirical modeling of layered integrated water vapor using surface mixing ratio in nigeria. J. Appl. Meteor. Climatol. 48 (2), 369–380.

Adeyemi, B., Emmanuel, I., 2011. Monitoring tropospheric radio refractivity over Nigeria using CM-SAF data derived from NOAA-15, 16 and 18 satellites. Indian J. Radio Space Phys. 40 (6), 301–310.

Arora, P.N., Arora, S., Arora, S., Arora, A., 2012. Comprehensive Statistical Methods 4th ed.. S. Chand and Company Pvt. Ltd..

Ayoade, J.O., 1983. Introduction to climatology for the tropics. Spectrum Books Limited.

Bevis, M., Businger, S., Chiswell, S., Herring, T.A., Anthes, R.A., Rocken, C., Ware, R.H., 1994. Gps meteorology: mapping zenith wet delays onto precipitable water. J. Appl. Meteorol. 33 (3), 379–386.

Boccaletti, S., Kurths, J., Osipov, G., Valladares, D.L., Zhou, C.S., 2002. The synchronization of chaotic systems. Phys. Rep. 366, 1–101.

CCIR, 1986. Radio meteorological data (propagation in non-ionized media). Tech. Rep. XVI, International Telecommunication Union Radiocommunication.

Das, D., Maitra, A., 2012. Time series prediction of rain rate during rain events at a tropical location. IET Microw., Antennas Propag. 6 (September), 1710–1716, ⟨http://dx.doi.org/10.1049/iet-map.2012.0338⟩.

Dee, D.P., Uppala, S.M., Simmons, A.J., Berrisford, P., Poli, P., Kobayashi, S., Andrae, U., Balmaseda, M.A., Balsamo, G., Bauer, P., Bechtold, P., Beljaars, A.C.M., Berg, L.V.D., Bidlot, J., Bormann, N., Delsol, C., Dragani, R., Fuentes, M., Geer, A.J., 2011. The ERA-interim reanalysis: configuration and performance of the data assimilation system. Q. J. R. Meteorol. Soc. 137 (656), 553–597.

Emmanuel, I., Adedayo, K., Ojo, O., 2015. Spatio-temporal variability of water vapour density over nigeria using cm saf data. Adv. Phys. Theor. Appl. 47, 23.

Freeman, J.R., 1983. Granger causality and the times series analysis of political relationships. Am. J. Political Sci. 27 (2), 327–358, ⟨http://www.jstor.org/stable/2111021⟩.

Granger, C.W.T., 1969. Investigating causal relations by econometric models and cross-spectral methods. Econometrica 37 (3), 424–438.

Hogg, D., Guiraud, F., Decker, M., 1981. Measurement of excess radio transmission length on earth-space paths. Astron. Astrophys. 95, 304–307.

ITU-R, 1997. The radio refractivity index: its formula and refractivity data. Tech. Rep. Rec. ITU-R P453, International Telecommunication Union Radiocommunication.

Kof, A.K., Gosset, M., Zahiri, E., Ochou, A.D., Kacou, M., Cazenave, F., Assamoi, P., 2014. Evaluation of X-band polarimetric radar estimation of rainfall and rain drop size distribution parameters in West Africa. Atmos. Res. 143, 438–461.

Legates, D.R., McCabe, G.J., 1999. Evaluating the use of "goodness-of-fit" measures in hydrologic and hydroclimatic model validation. Water Resour. Res. 35 (1), 233–241, ⟨http://dx.doi.org/10.1029/1998WR900018⟩.

Maity, R., 2012. Probabilistic assessment of one-step-ahead rainfall variation by Split Markov Process. Hydrol. Process. 26 (21), 3182–3194.

Majumdar, K., 2006. A new measure of phase synchronization for a pair of time series and seizure focus localization, 22 (December). URL ⟨http://arxiv.org/abs/nlin/0612032⟩

Marwan, N., Romano, M.C., Thiel, M., Kurths, J., 2007. Recurrence plots for the analysis of complex systems. Phys. Rep. 438, 237–329.

Midya, S.K., Ghosh, D., Das, G.K., Sarkar, H., 2013. Study of atmospheric refractivity prior to squall onset and its strong association with surface temperature and relative humidity over kolkata (22°34′n, 88°22′e). Indian J. Phys. 87 (9), 847–854.

Ogunjo, S., 2015. Effect of data transformation on long term memory of chaotic time series. Afr. Rev. Phys. 10, 219–224.

Ogunjo, S.T., 2013. Increased and reduced order synchronization of 2D and 3D dynamical systems. Int. J. Nonlinear Sci. 16 (2), 105–112.

Ogunjo, S.T., Adediji, A.T., Dada, J.B., 2015. Investigating chaotic features in solar radiation over a tropical station using recurrence quantification analysis. Theor. Appl. Climatol., URL ⟨http://dx.doi.org/10.1007/s00704-015-1642-4⟩.

Ogunjo, S.T., Ajewole, M.O., Adediji, A.T., Ojo, J.S., 2014. Predicting radio refractivity using a stochastic model. In: URSIGASS 2014, pp. 5–8. URL ⟨http://dx.doi.org/10.1109/URSIGASS.2014.6929637⟩

Ojo, J.S., Ajewole, M.O., Adediji, A.T., 2010. Estimation of cross-polarization due to rain over some stations in Nigeria. In: NURS 2010, pp. 154–159.

Ojo, K., Ogunjo, S.T., 2012. Synchronization of 4D Rabinovich hyperchaotic systems for secure communication. J. Niger. Assoc. Math. Phys. Math. Phys. 21, 35–44.

Ojo, K.S., Njah, A., Ogunjo, S.T., 2013a. Comparison of backstepping and modified active control in projective synchronization of chaos in an extended Bonhoffer van der Pol oscillator. Pramana 80 (5), 825–835, ⟨http://link.springer.com/article/10.1007/s12043-013-0526-3⟩.

Ojo, K.S., Njah, A., Ogunjo, S.T., Olusola, O.I., 2014a. Reduced order function projective combination synchronization of three josephson junctions using backstepping technique. Nonlinear Dyn. Syst. Theory 14 (2), 119.

Ojo, K.S., Njah, A., Ogunjo, S.T., Olusola, O.I., 2014b. Reduced order hybrid function projective combination synchronization of three Josephson junctions. Arch. Control Sci. 24 (1), 99–113, ⟨http://www.degruyter.com/view/j/acsc.2014.24.issue-1/acsc-2014-0007/acsc-2014-0007.xml⟩.

Ojo, K.S., Ogunjo, S.T., Njah, A.N., Fuwape, I.A., 2014c. Increased-order generalized synchronization of chaotic and hyperchaotic systems. Pramana 84 (1), 1–13.

Ojo, K.S., Ogunjo, S.T., Williams, O., 2013b. Mixed tracking and projective synchronization of 5D hyperchaotic system using active control. Cybern. Phys. 2 (1), 31–36, (2013 2, 31–36. ⟨http://adsabs.harvard.edu/abs/2013CyPh...0.2...31O⟩).

Olsen, R.L., Rogers, D.V., Hodge, D.B., 1978. The ar^b relation in the calculation of rain attenuation. IEEE Trans. Antennas Propag. AP-26 (2), 318–329.

Pecora, T.M., Carroll, T.L., 1990. Synchronization in chaotic systems. Phys. Rev. Lett. 64, 821–824.

Pikovsky, A., Rosenblum, M., Kurths, J., 2003. Synchronization: A Universal Concept in Nonlinear Sciences 12. Cambridge University Press.

Raju, C.S., Saha, K., Thampi, B.V., Parameswaran, K., 2007. Empirical model for mean temperature for Indian zone and estimation of precipitable water vapor from ground based GPS measurements. Ann. Geophys. 25, 1935–1948.

Reitan, C.H., 1963. Surface dew point and water vapor aloft. J. Appl. Meteorol. 2, 776–779.

Sharifi, M.B., Georgakakos, K.P., Rodriguez-Iturbe, I., 1990. Chaos in storm rainfall.pdf. J. Atmos. Sci. 47 (7), 888.

Shirer, H.N., Fosmire, C.J., Wells, R., Suciu, L., 1997. Estimating the correlation dimension of atmospheric time series. J. Atmos. Sci. 54 (1), 211–230.

Solheim, F.S., Vivekanandan, J., Ware, R.H., Rocken, C., 1999. Propagation delays induced in gps signals by dry air, water vapor, hydrometeors, and other particulates. J. Geophys. Res. 104 (D8), 9663–9670.

Tetens, O., 1930. Ber einige meteorologische begriffe. Z. Geophys. 6, 297–309.

Yang, S., Zou, X., 2012. Assessments of cloud liquid water contributions to gps radio occultation refractivity using measurements from cosmic and cloudsat. J. Geophys. Res. 117, D06219.